Journal of Physics D:
Applied Physics

PAPER

Fast-response IWO/Si heterojunction photodetectors

To cite this article: Xiaochuang Dai *et al* 2025 *J. Phys. D: Appl. Phys.* **58** 165102

IOP Publishing Journal of Physics D: Applied Physics

J. Phys. D: Appl. Phys. **58** (2025) 165102 (5pp) https://doi.org/10.1088/1361-6463/adbb79

Fast-response IWO/Si heterojunction photodetectors

Xiaochuang Dai, Jianwen Yang*, Huishan Wang, Yunxi Luo, Jinying Zeng, Wangzhou Shi* and Feng Liu*

Department of Physics, Shanghai Normal University, Shanghai 200234, People's Republic of China

E-mail: yangjianwen@shnu.edu.cn, wzshi@shnu.edu.cn and fliu@shnu.edu.cn

Received 20 December 2024, revised 15 February 2025
Accepted for publication 28 February 2025
Published 10 March 2025

Abstract

Indium tungsten oxide (IWO)/Si-based heterojunction photodetectors are designed with optimized structure, and they exhibit enhanced photoelectric detection capabilities. Under the action of the self-built electric field, the current easily flows from IWO to Si, but the resistance is high when flowing in the reverse direction due to the presence of the electron barrier. Under the 450 nm illumination condition, the effect of light on the forward flow from IWO to Si is minimal, but the illumination is sufficient to generate a large number of photogenerated carriers, which separate under the action of the built-in electric field and form a distinct photocurrent under the applied bias voltage. The optimized device exhibited ultra-fast response times (rise time of 8.2 ms and fall time of 7.9 ms), along with a high normalized detectivity ($D^* = 4.73 \times 10^{11}$ cm·Hz(1/2)/W) and a high photoswitch ratio (PS $= 6.6 \times 10^3$). These results demonstrate that the IWO/Si photodetector can serve as a high-performance photodetection device and is one of the candidates that exhibit more easily reproducible and stable performance compared to photodetectors based on two-dimensional materials.

Keywords: photodetectors, indium tungsten oxide, heterojunction, visible light, sputtering

1. Introduction

Photodetectors play a crucial role in industrial production, healthcare, medical imaging, night vision technology, national defense early warning systems, UV communication, space science, environmental monitoring [1–5]. As the demand for high-performance optoelectronic materials continues to grow, researchers are dedicated to developing new materials and devices with superior photoelectric performance. Heterostructures have been widely adopted in photodetectors due to their ability to enhance light absorption efficiency, sensitivity, and response speed, as well as to broaden the spectral response range [6]. Additionally, the built-in electric field in heterojunctions facilitates the separation of photogenerated carriers and suppresses their recombination, thereby improving device response speed and reducing dark current. Si-based heterojunctions are cost-effective and compatible with existing semiconductor technologies [7, 8]. While 2D material/Si heterojunctions (e.g. MoS_2/Si) suffer from instability and complex fabrication [9, 10], Oxide/Si devices combine high reproducibility, stability, and scalable sputtering deposition. As a transparent conductive oxide material with advantages such as high mobility, high uniformity, and the ability to be deposited at low temperatures [11, 12], indium tungsten oxide (IWO) offers adjustable bandgap and work function via W doping [13, 14], enabling optimized band alignment with Si. Although there have been numerous studies on various Si-based heterojunction photodetectors, such as NiO/Si[15], MoS_2/Si [16, 17], Bi/Si [18], PEDOT:PSS/Si [19], In_2Se_3/Si [2], V_2O_5/Si [20], graphene/n-Si [21], and p-Mn_2O_3/n-Si [22], rapid-response photoelectric detectors with response times on the order of several milliseconds are relatively rare. This study identified the optimal structure for

* Authors to whom any correspondence should be addressed.

IWO/Si-based heterojunction photodetectors and elucidated its working mechanism. Subsequently, we examined the visible spectrum ranging from 405 nm to 635 nm and found that under 450 nm illumination, the rapid rise/fall response times ($T_r = 8.2$ ms, $T_d = 7.9$ ms) indicated highly efficient photodetection performance.

2. Experimental

The flow chat of the photodetector fabrication process is shown in figure 1. N-type silicon substrates, cut to dimensions of 1×1 cm^2, were cleaned by successive immersion in acetone, ethanol, and deionized water under ultrasonic stirring for 10 min each step, followed by drying with argon. These cleaned substrates were then placed in an ion beam sputtering apparatus, where they underwent a 10 min sputtering process using an IWO target composed of WO_3 (3%) and In_2O_3 (97%) to deposit onto the Si substrates. The process began with the ion beam chamber being evacuated to 3.0×10^{-4} Pa to eliminate interference from other gases, followed by the introduction of Ar at a pressure of 6.5×10^{-2} Pa and a flow rate of 7.5 sccm, maintaining a distance of 22 cm from the target. After deposition, the films were thermally annealed in a tube furnace using a heating ramp of 2.67 °C min^{-1} to reach target temperatures of 300 °C, holding at each temperature for 2 h. Subsequently, the annealed samples were reinserted into the ion beam sputtering apparatus under the same conditions (6.5×10^{-2} Pa vacuum and 7.5 sccm argon flow) for another 10-minute sputtering session using a nickel (Ni) target to fabricate Ni electrodes on top of the IWO layer. The device pattern was achieved by covering the sample surface with a mask plate during the ion beam deposition of IWO and Ni, with the electrode spacing set at 4 millimeters.

The IWO and Ni films were deposited using the Dual Ion Beam Deposition equipment (SIBD4-5) produced by Seinan Industries Co., Ltd, which is equipped with two KRI Kaufman Source Controllers (KDC75 and KDC40). The photoelectric performance of the fabricated IWO/Si heterojunction devices was meticulously evaluated through current–voltage (I–V) characterization using a semiconductor parameter analyzer (Keysight B2902A), ensuring precise measurement of their optoelectronic properties.

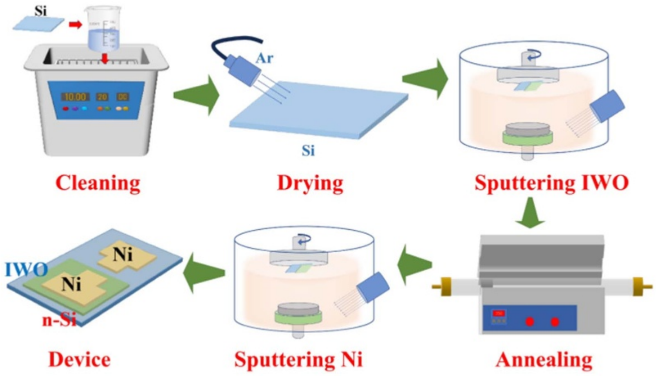

Figure 1. Flow chat of the photodetector fabrication process.

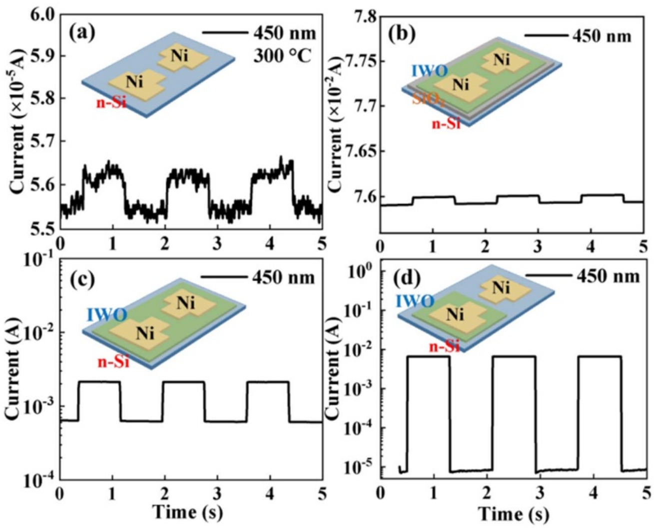

Figure 2. Photodetectors with different structures and their photodetection characteristics for 450 nm light (5 mW, IWO side electrode bias: −5 V).

3. Results and discussion

Figure 2 provides schematic diagrams of four different structures (inset) and their current-time response curves at a 300 °C annealing temperature (figures 2(a)–(d)). The photoelectric response efficiency of the Si conductivity-type photodetector is very low, as shown in figure 2(a). After the insertion of the IWO interlayer, the photoelectric response is significantly improved, as shown in figure 2(c). The presence of the IWO thin film results in more stable current-time response curves and higher photocurrents. To verify whether it is the Si/IWO or the IWO/Ni that influences the photoelectric characteristics, an Ni/IWO/Ni photodetector was fabricated on a Si-SiO_2 substrate, as shown in figure 2(b). As can be seen from the Figure, without the influence of Si, the Ni/IWO/Ni photodetector does not exhibit good photodetector performance, and there is little change in the current between the on and off states. Figures 2(c) and (d) compare the photoelectric characteristics of the Ni/IWO-Si/Ni symmetric structure with the Ni/IWO/Si/Ni heterojunction structure. From the comparison, it can be concluded that the IWO/Si heterojunction structure has a significant impact on the excellent detection properties of the Ni/IWO/Si/Ni photodetector. It exhibits a high photocurrent and a low dark current, with a large on-off ratio. Additionally, the response time of the device is also on the order of milliseconds.

To further explain the working mechanism of the IWO/n-Si based heterojunction, figure 3(a) provides the energy band diagram of the IWO/Si heterojunction structure. The electron transfer at the n-n type heterojunction interface is facilitated by the difference in work functions (Φ) of IWO and Si [23, 24]. Even though there's a slight difference in composition, previous literature reports that the band gaps for IWO and n-Si are roughly 3.86 eV and 1.12 eV, and their electron affinities are listed as 4.3–4.7 eV and 4.05 eV, respectively [25–28]. When the two materials come into contact, electrons flow from Si

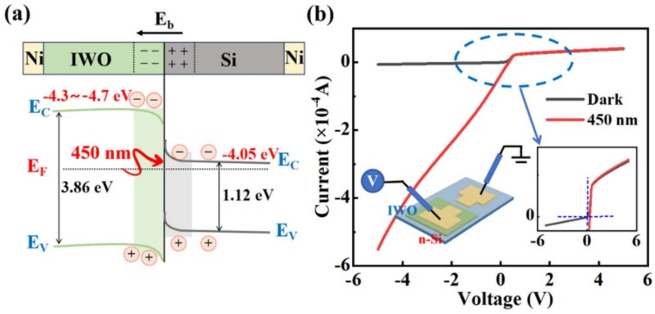

Figure 3. (a) Band diagram of the IWO/Si heterojunction, (b) the unidirectional conductivity of the IWO/Si diode with IWO side electrode bias ranging from −5 to 5 V bias under 5 mW power 450 nm wavelength irradiation.

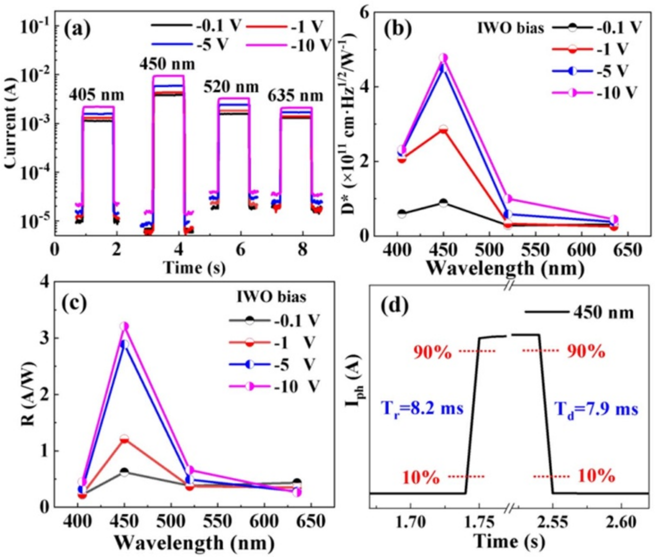

Figure 4. (a) The current time response curve, the normalized (b) D^* and (c) R values of the IWO/Si photodetector under various light wavelengths (405–635 nm, 5 mW)and different IWO bias voltages, and (d) the typical rise/fall response time.

to IWO until the Fermi levels align to achieve thermal equilibrium. Positive charges remain on the n-type Si side, while negative charges accumulate on the IWO side. These space charge regions create an internal electric field (E_b) directed from n-type Si to IWO (figure 3(a)). Due to the presence of the energy barrier, it is easy for the current to flow from IWO to Si, but the resistance is very high when flowing in the reverse direction due to the presence of the electron potential barrier, which can be seen in figure 3(b) under dark conditions. Under the condition of 450 nm light illumination, the effect of light on the forward current flow from IWO to Si is small. In contrast, under reverse bias, the carrier depletion region expands, and the photogenerated electron-hole pairs, under the action of the built-in electric field, cause the electrons to flow towards the Si and the holes towards the IWO. These carriers, under the influence of the external bias, create a photogenerated current, resulting in a clear photoelectric response.

Subsequently, the photoelectric response characteristics of the IWO/Si photodetector under different illumination wavelengths (405–635 nm) and different IWO bias voltages are analyzed, as shown in figure 4(a). The spot radius of the circular laser is 1 mm, and the power is 5 mW. The corresponding specific detectivity (D^*) and responsivity (R) values are depicted in figures 4(b) and (c), respectively. By exploring the current-time response performance, it was found that the optimal response occurred at a wavelength of 450 nm. Given that the energy of a photon with a wavelength of 450 nm is roughly 2.76 eV, this could correspond to the energy difference between the top of the valence band in IWO and the bottom of the conduction band in n-Si within the heterostructure. The R is defined as the efficiency of generating current per unit of incident light power, and can be expressed as:

$$R = \frac{I_{\mathrm{Ph}}}{P_{\mathrm{in}}} \quad (1)$$

where P_{in} represents the optical power. The photoswitching ratio (PS), another key parameter, reflects the device's modulation capability between high and low current states under illumination, and can be expressed as:

$$PS = \frac{I_{\mathrm{on}}}{I_{\mathrm{off}}} \quad (2)$$

where I_{on} is the current under illumination and I_{off} is the current in darkness. As a critical parameter for evaluating the performance of a photodetector, the D^* represents the smallest amount of optical power that the detector can detect. The D^*, assuming that shot noise from dark current is the primary contributor to the total noise, is defined by the following equation [29]:

$$D^* = \frac{\sqrt{A}\cdot R}{\sqrt{2qI_{\mathrm{off}}}} \quad (3)$$

where A represents the detection area and q denotes the electronic charge. The calculated R of the IWO/Si photodetector under 450 nm illumination (−10 V IWO bias) is 3.19 A W^{-1}, it can be inferred that the device possesses a strong capability for photocurrent conversion, which is crucial for applications requiring precise detection of light signals and their conversion into electrical signals. The corresponding D^* value for this device is 4.73 × 10^{11} cm·Hz$^{(1/2)}$/W, indicating its suitability for high-sensitivity applications with an excellent signal-to-noise ratio. A significant PS of 6.6 × 10^3 indicates that the device can reliably differentiate between different current levels, with minimal overlap ensuring clear distinction between active and inactive states. Additionally, response time, as a critical parameter for evaluating the sensitivity and efficiency of a photodetector, includes rise time and fall time. Rise time refers to the duration required for the photocurrent to increase from 10% to 90% of its maximum value after exposure; fall time is defined as the duration for the photocurrent to decrease from 90% to 10% of its peak value after the light source is removed. The typical rise time of the IWO/Si photodetector is 8.2 ms, and the fall time is 7.9 ms (as shown in figure 4(d)), indicating that the device can rapidly respond to light signals, thereby providing potential application possibilities for optical communication systems and rapid detection.

Table 1. The reported photodetectors related to In_2O_3/WO_3.

Structure	Bias (V)	λ (nm)	R (A W^{-1})	D^* (cm·$Hz^{(1/2)}$/W)	Rise/fall time	Year	References
WO_3/InO_3 Nanocluster	3	—	290.49	5.97×10^{13}	0.89/0.81 s	2019	[30]
In_2O_3 Nanosheets	—	254	0.17236	4.43×10^{11}	0.8/2.2 s	2022	[31]
InWO	−10	—	160	—	35/38 s	2024	[32]
Porous In_2O_3	3	254	8.16×10^{-2}	—	15/18 ms	2024	[33]
IWO/Si	−10	450	3.19	4.73×10^{11}	8.2/7.9 ms	2025	This work

Table 1 lists the reported photodetectors related to In_2O_3/WO_3, include WO_3-InO_3 nanocluster [30], In_2O_3 nanosheets [31], InWO [32], porous In_2O_3 [33], and IWO/Si(This work). It can be seen from the table that the photoelectric response times are mostly on the order of seconds. In contrast, the photodetector prepared in this paper exhibits an fast response characteristic, which is very beneficial for the rapid response of the device and will further enhance the detection sensitivity of the photodetector. It proves apt for avant-garde optoelectronic applications spanning smart security systems, digital displays, and advanced sensing technologies.

4. Conclusion

The photodetector, which has received performance enhancement based on the IWO/Si heterojunction structure, has been fabricated and demonstrated, exhibiting excellent photoelectric response characteristics. The asymmetric conductivity of the IWO/Si heterojunction is beneficial for photodetection, and the photovoltaic response is more pronounced during reverse conduction. Besides, the photodetector shows different detection characteristics for different visible light wavelengths. Compared to previous reports, the IWO/Si heterojunction photodetector has the advantages of millisecond fast response time and high detectivity, potentially becoming one of the candidate devices for fast detection equipment. The optimized photodetector (−10 V IWO bias) exhibited peak responsiveness at a wavelength of 450 nm with the current switch ratio 6.6×10^3, the detectivity D^* 4.73×10^{11} cm·Hz(1/2)/W, the responsivity R 3.19 A W^{-1}. The typical rise time T_r is 8.2 ms, and the fall time T_d is 7.9 ms.

Data availability statement

All data that support the findings of this study are included within the article (and any supplementary files).

Acknowledgment

This work was supported by Program of Shanghai Academic Research Leader under Grant 22XD1422100, National Natural Science Foundation of China (Nos. 61904108, 12141303, 12073018, 12373099, U1931205), 'Chenguang Program' (No. 19CG50) by Shanghai Education Development Foundation and Shanghai Municipal Education Commission, Shanghai Local College Capacity Building Project (No. 21010503200).

ORCID iDs

Xiaochuang Dai https://orcid.org/0009-0002-6433-1338
Jianwen Yang https://orcid.org/0000-0002-9565-2380
Yunxi Luo https://orcid.org/0009-0009-8957-357X

References

[1] Barrera L, Layne B W, Chen Z, Watanabe K, Kudo A, Esposito D V, Ardo S and Chandran R B 2024 Revealing the role of redox reaction selectivity and mass transfer in current–voltage predictions for ensembles of photocatalysts *Energy Environ. Sci.* **17** 8254–73

[2] Jia C, Wu S, Fan J, Luo C, Fan M, Li M, He L, Yang Y and Zhang H 2023 Ferroelectrically modulated and enhanced photoresponse in a self-powered α-In_2Se_3/Si heterojunction photodetector *ACS Nano* **17** 6534–44

[3] He H, Liu J, Chen S, Niu C, Zhang X, Jia J, Wu C, Hu H, Wu F and Guo D 2024 A general strategy for enhancing the performance of Ga_2O_3-based self-powered solar-blind photodetectors through band structure engineering *J. Appl. Phys.* **58** 065104

[4] Liu X, Yang X, Tang Q, Lv Y, Zhang G and Feng W 2024 Application and prospect of 2D materials in photodetectors *J. Appl. Phys.* **57** 305401

[5] Liu Z and Tang W 2023 A review of Ga_2O_3 deep-ultraviolet metal–semiconductor Schottky photodiodes *J. Appl. Phys.* **56** 093002

[6] Huo N and Konstantatos G 2018 Recent progress and future prospects of 2D-based photodetectors *Adv. Mater.* **30** 1801164

[7] Şakar B C, Orhan Z, Yıldırım F and Aydoğan Ş 2022 Ultraviolet and visible photo-response of transparent conductive Al-doped ZnO (AZO)/n-Silicon isotype heterojunction device *J. Appl. Phys.* **55** 425107

[8] Zhang Y, Yang F, Guo Q, Feng X, Duan Y, Guo J, Cheng G and Du Z 2022 The self-powered photodetector of n-Si/n-ZnO heterojunction with enhanced temperature adaptability via transient current response *J. Appl. Phys.* **55** 504004

[9] Kumar A, Khan M A and Kumar M 2021 Recent advances in UV photodetectors based on 2D materials: a review *J. Appl. Phys.* **55** 133002

[10] Zhang S, Liu J, Kirchner M M, Wang H, Ren Y and Lei W 2021 Two-dimensional heterostructures and their device applications: progress, challenges and opportunities *J. Appl. Phys.* **54** 433001

[11] Yang J, Ren J, Lin D, Han Y, Qu M, Pi S, Fu R and Zhang Q 2017 Amorphous nickel incorporated tin oxide thin film transistors *J. Phys. D: Appl. Phys.* **50** 355103

[12] Yang J, Meng T, Yang Z, Cui C and Zhang Q 2015 Investigation of tungsten doped tin oxide thin film transistors *J. Phys. D: Appl. Phys.* **48** 435108

[13] Aikawa S, Darmawan P, Yanagisawa K, Nabatame T, Abe Y and Tsukagoshi K 2013 Thin-film transistors fabricated by low-temperature process based on Ga-and Zn-free

amorphous oxide semiconductor *Appl. Phys. Lett.* **102** 102101
[14] Choi D-H, Seok H-J, Kim S-K and Kim H-K 2024 Highly transparent and conductive Ga-doped InWO multi-component electrodes for perovskite photovoltaics *J. Alloys Compd.* **1001** 175018
[15] Ahmed A A, Hashim M, Qahtan T F and Rashid M 2022 Preparation and characteristics study of self-powered and fast response p-NiO/n-Si heterojunction photodetector *Ceram. Int.* **48** 20078–89
[16] Wang L, Jie J, Shao Z, Zhang Q, Zhang X, Wang Y, Sun Z and Lee S T 2015 MoS_2/Si heterojunction with vertically standing layered structure for ultrafast, high-detectivity, self-driven visible–near infrared photodetectors *Adv. Funct. Mater.* **25** 2910–9
[17] Dhyani V and Das S 2017 High-speed scalable silicon-MoS_2 PN heterojunction photodetectors *Sci. Rep.* **7** 1–9
[18] Yao J, Zheng Z, Shao J and Yang G 2015 Promoting photosensitivity and detectivity of the Bi/Si heterojunction photodetector by inserting a WS_2 layer *ACS Appl. Mater. Interfaces* **7** 26701–8
[19] Liang Z, Zeng P, Liu P, Zhao C, Xie W and Mai W 2016 Interface engineering to boost photoresponse performance of self-powered, broad-bandwidth PEDOT: PSS/Si heterojunction photodetector *ACS Appl. Mater. Interfaces* **8** 19158–67
[20] Fu Y, Liu Y, Ma K, Ji Z, Mai W and Zhao C 2020 Interfacial engineering to boost photoresponse performance and stability of V_2O_5/n-Si heterojunction photodetectors *J. Alloys Compd.* **819** 153063
[21] Li X, Zhu M, Du M, Lv Z, Zhang L, Li Y, Yang Y, Yang T, Li X and Wang K 2016 High detectivity graphene-silicon heterojunction photodetector *Small* **12** 595–601
[22] Kadhm A J, Ismail R A and Atwan A F 2022 Fabrication of visible-enhanced nanostructured Mn_2O_3/Si heterojunction photodetector by rapid thermal oxidation *Silicon* **14** 5297–310
[23] Vishnuraj R, Unnathpadi R, Rangarajan M and Pullithadathil B 2024 n–n type In_2O_3@-WO_3 heterojunction nanowires: enhanced NO_2 gas sensing characteristics for environmental monitoring *Mikrochim. Acta* **191** 645
[24] Dillon J A and Farnsworth H E 1958 Work function and sorption properties of silicon crystals *J. Appl. Phys.* **29** 1195–202
[25] Han C, Santbergen R, van Duffelen M, Procel P, Zhao Y, Yang G, Zhang X, Zeman M, Mazzarella L and Isabella O 2022 Towards bifacial silicon heterojunction solar cells with reduced TCO use *Prog. Photovolt., Res. Appl.* **30** 750–62
[26] Liu W, Zhang L, Cong S, Chen R, Wu Z, Meng F, Shi Q and Liu Z 2018 Controllable a-Si: h/c-Si interface passivation by residual SiH_4 molecules in H_2 plasma *Sol. Energy Mater. Sol. Cells* **174** 233–9
[27] Jiao B-C, Zhang X-D, Wei C-C, Huang Q, Chen X-L and Zhao Y 2013 Improving electrical performance of ultrasonic spray pyrolysis grown textured ZnO films by introducing In2O3: w interface layer *Appl. Surf. Sci.* **279** 464–71
[28] Fan W-T, Liu P-T, Kuo P-Y, Chang C-M, Liu I-H and Kuo Y 2021 Numerical analysis of oxygen-related defects in amorphous In-WO nanosheet thin-film transistor *Nanomaterials* **11** 3070
[29] Deng M, Li Z, Deng X, Hu Y and Fang X 2023 Wafer-scale heterogeneous integration of self-powered lead-free metal halide UV photodetectors with ultrahigh stability and homogeneity *J. Mater. Sci. Technol.* **164** 150–9
[30] Ngangbam C, Rajkumari R, Thoibileima L, Alam M W and Singh N K 2021 High responsivity of GLAD synthesized isotype WO_3/In_2O_3 nanocluster *IEEE Photonics Technol. Lett.* **33** 943–6
[31] Zhang M, Yu H, Li H, Jiang Y, Qu L, Wang Y, Gao F and Feng W 2023 Ultrathin In_2O_3 nanosheets toward high responsivity and rejection ratio visible-blind UV photodetection *Small* **19** 2205623
[32] Lam K-T, Donald A, Chang S-P, Kuan C-Y and Chang S-J 2024 Fabrication and properties of tungsten-doped indium oxide ultraviolet photodetector *Sens. Mater.* **36** 1835
[33] Zhang N, Gao X, Guan H, Sun S, Liu J, Shao Z, Gao Q, Zhang Y, Sun R and Yang G 2024 Three-dimensional porous In_2O_3 arrays for self-powered transparent solar-blind photodetectors with high responsivity and excellent spectral selectivity *Nano Res.* **17** 4471–7